

EarthGPT-X: Enabling MLLMs to Flexibly and Comprehensively Understand Multi-Source Remote Sensing Imagery

Wei Zhang, Miaoxin Cai, *Graduate Student Member, IEEE*, Yaqian Ning, Tong Zhang, *Graduate Student Member, IEEE*, Yin Zhuang[†] *Member, IEEE*, He Chen, *Member, IEEE*, Jun Li, *Fellow, IEEE*, and Xuerui Mao[†]

Abstract—Recent advances in the visual-language area have developed natural multi-modal large language models (MLLMs) for spatial reasoning through visual prompting. However, due to remote sensing (RS) imagery containing abundant geospatial information that differs from natural images, it is challenging to effectively adapt natural spatial models to the RS domain. Moreover, current RS MLLMs are limited in overly narrow interpretation levels and interaction manner, hindering their applicability in real-world scenarios. To address those challenges, a spatial MLLM named EarthGPT-X is proposed, enabling a comprehensive understanding of multi-source RS imagery, such as optical, synthetic aperture radar (SAR), and infrared. EarthGPT-X offers zoom-in and zoom-out insight, and possesses flexible multi-grained interactive abilities. Moreover, EarthGPT-X unifies two types of critical spatial tasks (i.e., referring and grounding) into a visual prompting framework. To achieve these versatile capabilities, several key strategies are developed. The first is the multi-modal content integration method, which enhances the interplay between images, visual prompts, and text instructions. Subsequently, a cross-domain one-stage fusion training strategy is proposed, utilizing the large language model (LLM) as a unified interface for multi-source multi-task learning. Furthermore, by incorporating a pixel perception module, the referring and grounding tasks are seamlessly unified within a single framework. In addition, the experiments conducted demonstrate the superiority of the proposed EarthGPT-X in multi-grained tasks and its impressive flexibility in multi-modal interaction, revealing significant advancements of MLLM in the RS field.

Index Terms—Multi-source, Spatial reasoning, Remote sensing (RS), Multi-modal large language models (MLLMs).

[†] Co-corresponding author: Yin Zhuang and Xuerui Mao.

Wei Zhang is with the Advanced Research Institute of Multidisciplinary Sciences, Beijing Institute of Technology, Beijing 100081, China, and also with the School of Mechatronical Engineering, Beijing Institute of Technology, Beijing 100081, China. (e-mail: w.w.zhanger@gmail.com)

Xuerui Mao is with the Advanced Research Institute of Multidisciplinary Sciences, Beijing Institute of Technology, Beijing 100081, China, and with the School of Mechatronical Engineering, Beijing Institute of Technology, Beijing 100081, China, and also with Yangtze Delta Region Academy of Beijing Institute of Technology, Jiaxing 314003, China. (e-mail: maoxuerui@sina.com).

He Chen, Yin Zhuang, Miaoxin Cai, and Tong Zhang are with the National Key Laboratory of Science and Technology on Space-Born Intelligent Information Processing, Beijing Institute of Technology, Beijing 100081, China. (e-mail: chenhe@bit.edu.cn, yzhuang@bit.edu.cn, 3120220667@bit.edu.cn, bit_zhangtong@163.com).

Yaqian Ning is with the School of Optics and Photonics, Beijing Institute of Technology, Beijing 100081, China. (e-mail: ningyq@bit.edu.cn).

Jun Li is with the School of Computer Science and Hubei Key Laboratory of Intelligent Geo-Information Processing, China University of Geosciences, Wuhan, 430078, China (e-mail: lijuncug@cug.edu.cn).

I. INTRODUCTION

TYPICAL spatial understanding tasks in multi-modal learning include *referring and grounding*, which essentially require aligning regions in the image with text semantics [1]. *Referring* aims to accurately generate the interpretation sequence of the specific areas. *Grounding* requires localizing the objects or rendering object segmentation masks based on the user’s language expression [2], [3]. Most recently, enabling multi-modal large language models (MLLMs) with comprehensive spatial understanding has become the focal of research in the natural scenarios [4]–[6]. However, these models struggle with the remote sensing (RS) imagery, which features multi-source, multi-viewpoint, and scale variations due to different imaging conditions [7]. Although current RS MLLMs can handle a wide range of RS visual tasks [8], [9], they primarily focus on holistic image understanding, lacking spatial perception. They solely rely on text instructions which can lead to ambiguity and limited context. It is indispensable for establishing a comprehensive and spatial-aware MLLM to interpret RS images under flexible interactions.

Notably, in the human world, people can achieve an all-around understanding of visual information, allowing for both zoom-in fine-grained analyses and zoom-out coarse-grained overviews [10]. Inspired by this, universal MLLM and multi-grained prompting learning have been extensively studied in the visual-language learning community [11]. Remarkable advances of MLLMs include close-source Open-AI’s GPT series [12]–[14], open-source Meta’s LLaMA series [15], [16], and parameter-efficient LLaMA-Adapter series [17], [18], which demonstrate versatile capabilities of handling multi-modal various visual tasks. On top of that, visual prompting models advance the field by injecting visual prompts beyond text instructions to enable multi-grained visual reasoning and enhance spatial perception [19]. Specifically, representative works comprise promptable segmentation model segment anything (SAM) [20], region-of-interest perception model GPT4RoI [4], refer-and-ground MLLM Ferret [1], etc. However, the aforementioned models are tailored for the natural imagery, it is challenging to directly adapt them to the diverse RS data.

Limited efforts in the RS domain have been made to enhance spatial understanding. A key example is RSPrompter [21], which is based on SAM and develops an automated prompts generation approach to facilitate interactive

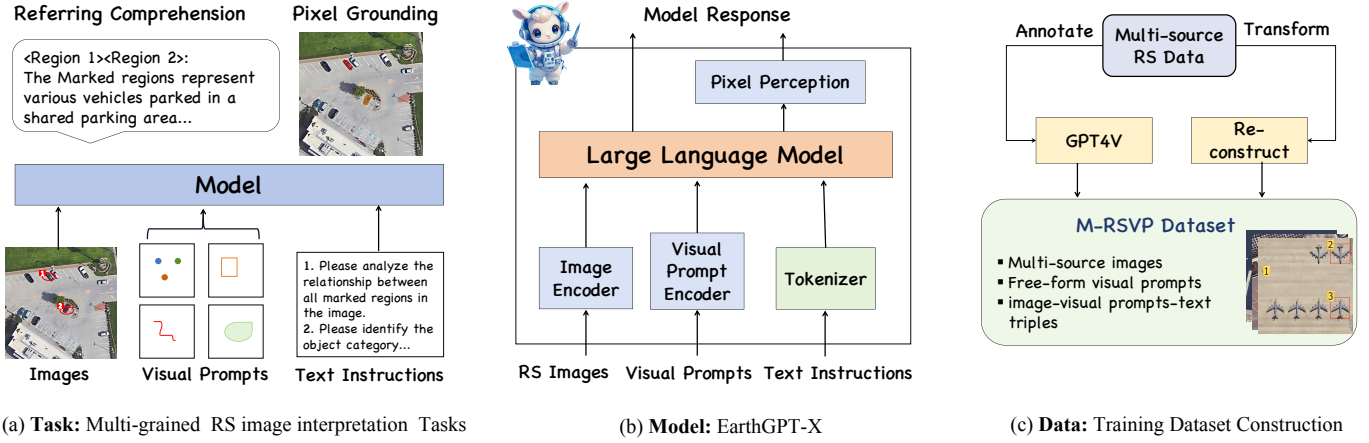


Fig. 1. An overview of the proposed flexible and comprehensive spatial understanding framework for RS imagery: (a) **Task**: various multi-grained referring and grounding tasks; (b) **Model**: the proposed model consists of an image encoder, a visual prompts encoder, a text tokenizer, a LLM, and a pixel perception module; (c) **Data**: the training dataset M-RSVP is transformed based on existing multi-source RS data including optical, SAR, and infrared.

segmentation. However, RSPrompter is only designed for instance segmentation. RSVG [2] defines the visual grounding tasks in the RS domain and can locate the referred objects using boxes under natural language expression. Recent notable works, such as EarthGPT [8] and Geochat [9], have realized RS holistic and regional imagery comprehension under the unified visual-language learning framework, facilitating the development of MLLMs in the RS domain. Nevertheless, RSVG, EarthGPT, and Geochat solely support language interaction without visual prompts to realize referring expression comprehension. Notably, EarthMarker [22] is constructed as the first visual prompting learning framework in the RS domain and is capable of region-level and point-level RS imagery interpretation. Regrettably, EarthMarker is mainly oriented towards optical images and lacks support for multi-source imagery and free-form visual prompts, hampering flexible human-AI interaction and comprehensive understanding of RS data. Thus, the study on enabling MLLMs to flexibly interpret multi-source RS images at any granularity remains in its infancy stages.

To resolve the limitations of existing models and draw inspiration from how humans understand multi-modal, multi-grained information through flexible interactions, a spatial MLLM named EarthGPT-X is proposed based on visual prompt learning. EarthGPT-X is designed for a comprehensive understanding of multi-source RS imagery under flexible visual prompts (e.g., points, boxes, circles, and scribbles), and unifying *referring and grounding* tasks within a free-form region-text alignment architecture. As depicted in Fig. 1, the EarthGPT-X architecture consists of three interconnected components: multi-grained RS image interpretation *tasks*, a visual prompting *model*, a construction pipeline of training *datasets*. Specifically, EarthGPT-X not only allows for zoom-in fine-grained reasoning (e.g., free-form region captioning, referring object classification, and object inter-relationship analyses), but also supports zoom-out coarse-grained tasks (e.g., image-level captioning, scene classification). Secondly, the key of the model is to realize multi-modal content integration including images, visual prompts, and text instructions. The multi-modal

signals are then fed into the large language models (LLM) for subsequent mixed tuning. Additionally, to unify referring and grounding in a single framework, the pixel perception module is designed to generate binary segmentation masks related to referring objects. Thirdly, the training dataset named M-RSVP is constructed, transforming from existing multi-source datasets, which is uniformly reorganized and relabeled as *image-visual prompts-text* triples, with a portion re-annotated using GPT-4V [23] to support the generation of longer and more detailed descriptions [22].

In addition, observed that existing synthetic aperture radar (SAR) and infrared datasets are limited to object detection tasks, which are insufficient for developing complex visual reasoning capabilities of MLLMs. To address this shortcoming, the multi-domain data are integrated for generalizing general-domain knowledge into SAR and infrared scenarios. Furthermore, to allow for free-form visual prompts data, a noise augmentation method is proposed to add noise that either partially covers the ground truth or extends beyond it to simulate free-form shapes. Based on the newly constructed training datasets, a one-stage all-in-one training strategy is proposed for mixed tuning, facilitating cross-domain data mutual learning and alleviating the need for manual effort for manually setting during the training.

To further investigate EarthGPT-X's superior comprehensive interpretation ability on multi-source imagery, we compare it with recent state-of-the-art (SOTA) natural and RS MLLMs. Impressively, EarthGPT-X can realize multi-source data reasoning accurately and provide a more comprehensive and detailed understanding of RS images. Furthermore, to evaluate the effectiveness of the EarthGPT-X's structure, we conduct ablation studies to assess the designed components' contributions to the overall performance. Experimental results demonstrate that the proposed EarthGPT-X not only achieves competitive performances on vision-language tasks, but also creates impressive results on referring and grounding tasks.

Our contributions can be summarized as follows.

- A *RS Multi-source Spatial MLLM*, *EarthGPT-X*. A pioneering MLLM named EarthGPT-X is proposed, specif-

ically designed for a comprehensive spatial understanding of multi-source RS imagery. EarthGPT-X advances existing RS MLLMs by enabling flexible multi-grained imagery interpretation, and offers zoom-in and zoom-out insight, powered by designed free-form visual prompts. Furthermore, EarthGPT-X unifies *referring and grounding* tasks into a visual prompting learning framework, facilitates an adaptable understanding of RS data, and represents a significant milestone in developing versatile MLLMs on RS scenarios.

- *First Multi-source Visual Instruction Dataset, M-RSVP.* A multi-source multi-modal visual-prompt-based instruction dataset named M-RSVP, comprising over 200 k *image-visual prompts-text* triples, is constructed. M-RSVP fills the gap of multi-source visual prompting data in the RS domain, facilitating a multi-grained understanding of RS imagery across various scenes, diverse sources, and varying imaging conditions.
- *Flexible Multi-modal Content Interaction.* A multi-modal content integration mechanism is developed, enhancing the mutual understanding between dense image representations, sparse visual prompt features, and text instruction embeddings. This mechanism leads to a deeper comprehension of the referring regions in holistic images. Moreover, by combining with a noise augmentation method for simulating free-form shapes, this mechanism endows the proposed EarthGPT-X with comprehensive RS imagery understanding under flexible human-AI interaction.
- *Cross-domain Knowledge Integration.* A cross-domain one-stage fusion training strategy is proposed, transferring and generalizing universal domain-level knowledge into SAR and infrared scenarios. This approach effectively mitigates the limitations of existing SAR and infrared data interpretation, which are typically restricted to object detection tasks and hinder the potential to perform complex multi-task visual reasoning. Furthermore, the one-stage all-in-one training facilitates cross-domain data mutual perception and reduces the reliance on extensive manual effort.

II. RELATED WORK

A. LLMs and MLLMs in Natural Scenarios

The rapid development of LLMs has significantly advanced natural language processing (NLP), demonstrating remarkable capabilities in diverse contexts. Specifically, GPT-3 [12] has demonstrated the power of large-scale models, containing billions to trillions of parameters. InstructGPT [24] and ChatGPT [13] have further enhanced this by showcasing remarkable fluency and adaptability in various conversational tasks. Impressively, the open-source community has significantly contributed to advancing LLMs, with resources like LLaMA series [25] enhancing the instruction-following capabilities of these models. Recent efforts, including Alpaca [26], Vicuna [27], and GPT-4-LLM [28], have introduced full fine-tuning techniques to effectively equip LLMs with robust instruction-following abilities. Additionally, LLaMA-Adapter [18] has demonstrated that parameter-efficient fine-

tuning can achieve comparable results with full parameter fine-tuning, offering a more efficient approach to model adaptation.

Notably, an essential step toward achieving general intelligence is integrating multi-modal perception into LLMs, allowing them to handle multi-modal data beyond text. Several works [29]–[32] focus on incorporating multi-modal inputs to support task-specific objectives across various modalities. Models like VisualGPT [29], BLIP [30], Flamingo [32], and Kosmos-1 [33] have shown strong multi-modal reasoning abilities by aligning LLMs with visual data. This alignment is achieved using techniques like projection layers, zero-shot attention mechanisms, and intermediate networks, as demonstrated by MiniGPT-4 [34], LLAMA-Adapter V2 [17], and mPLUG-Owl [35]. In addition, with multi-modal LLMs continuing to evolve, other modalities include audio, video [36], [37], and 3D point clouds [38]–[40] are being integrated into MLLMs.

B. MLLMs in RS Scenarios

Inspired by MLLMs in natural domains, MLLMs in the RS field have also made significant strides. Several pioneering RS MLLMs have emerged recently. For example, RSGPT [41], which fine-tunes Instruct-BLIP [42] on a high-quality image-text pairs dataset, demonstrates strong capabilities in image captioning and visual question answer (VQA). However, RSGPT struggles with other visual tasks including object classification and detection, lacking generalization abilities. A key advance is Geochat [9], which is the first versatile MLLM designed to solve multiple tasks for optical RS images. EarthGPT [8] introduces a universal MLLM capable of handling multi-source RS imagery and a broad range of RS visual tasks, and supports regional visual reasoning. In addition, another RS MLLM called LHRS-Bot [43] has established the LHRS-Bench to assist the RS community in evaluating RS-domain MLLMs across diverse evaluation metrics. These models have undoubtedly advanced the development of MLLMs within the RS-specific domain. Nevertheless, EarthGPT, Geochat, and LHRS-Bot solely allow language interaction in multi-turn conversations to handle visual tasks, and fail to support referring comprehension under visual prompt instruction, which restricts flexible interaction in real-world applications.

C. Prompting Learning

Prompt learning has emerged as a key area of research in NLP [12]. Notable works such as AutoPrompt [44] and CoOp [45] focus on automating prompt template generation for language and vision-language models, reducing the need for manual crafting. In parallel, language prompting has been applied to open-vocabulary detection models, including DetPro [46] and PromptDet [47]. While language prompting is well-developed, visual prompting remains underexplored. A significant advancement in this area is the SAM [20] model, which supports various segmentation prompts to improve zero-shot performance. However, SAM lacks object semantic labels, which is addressed by Semantic-SAM [48]. Moreover, models like GPT4RoI [4] and RegionBlip [5] leverage spatial boxes and combine language with region-of-interest input for

TABLE I
COMPARISONS OF EARTHGPT-X v.s. RECENT MLLMS IN RS DOMAIN.

Model	Text	Image		Visual Prompts			Pixel-level
	Instruction	Optical	Multi-source	Point	Box	Free-form	Grounding
RSGPT [41]	✓	✓	✗	✗	✗	✗	✗
RS-LLaVA [51]	✓	✓	✗	✗	✗	✗	✗
GeoChat [9]	✓	✓	✗	✗	✗	✗	✗
EarthGPT [8]	✓	✓	✓	✗	✗	✗	✗
Popeye [52]	✓	✓	✓	✗	✗	✗	✓
SkyEyeGPT [53]	✓	✓	✗	✗	✗	✓	✗
EarthMarker [22]	✓	✓	✗	✓	✓	✗	✗
EarthGPT-X	✓	✓	✓	✓	✓	✓	✓

regional recognition. Colorful Prompting Tuning (CPT) [49] uses color-based prompts to enhance MLLMs performance. Osprey [3] goes further by incorporating fine-grained mask regions into language instructions for pixel-level understanding. Ferret [1] is capable of understanding spatial referring of any shape or granularity within an image and accurately grounding open-vocabulary descriptions. Additionally, SPHINX-V [50] supports free-form visual prompts to achieve pixel-level image comprehension. Mentioned above models are designed for the natural domain.

Note that EarthMarker [22] stands as the pioneering visual prompting framework tailored for the RS domain, specifically designed to interpret RS imagery at both region and point levels. EarthMarker constructs a large-scale RS visual prompting dataset and leverages visual prompts learning to endow MLLM with region-level and point-level RS imagery interpretation capabilities. However, EarthMarker is primarily focused on optical images and lacks support for multi-source imagery and free-form visual prompts. This limitation significantly hinders its potential for flexible interactions and restricts its ability to provide a comprehensive understanding of the diverse and complex characteristics of RS data and broader applicability in real-world RS scenarios.

In summary, existing RS MLLMs have constructed the visual-language learning diagram to comprehend RS imagery and support language interaction in multi-turn dialogues. More advanced than existing MLLMs and EarthMarker, the proposed EarthGPT-X is designed for multi-source imagery comprehension using a dual-prompt system of text instructions and visual prompts. With free-form visual prompting, EarthGPT-X offers comprehensive and flexible visual perception. A straightforward side-by-side comparison of EarthGPT-X versus the recent RS MLLMs is shown in Tab. I.

III. METHODOLOGY

The goal is to unify the referring comprehension at any granularity and pixel grounding into a visual prompt framework in the multi-source RS scenarios. To this end, EarthGPT-X is developed to explore a more general and comprehensive

visual prompting learning paradigm. The entire EarthGPT-X framework is detailed in this section. Specifically, we first elaborate on the multi-modal content integration mechanism (Section III-A). Subsequently, the cross-domain one-stage fusion training strategy is presented (Section III-B). In addition, the pixel perception module is introduced in Section III-C.

A. Multi-modal Content Integration

The multi-modal input stream of the EarthGPT-X is characterized by its tripartite structure, comprising an image global and local perception module, a spatial-aware module, and a text instruction processing module. Those multi-modal content encoding and integration are detailed as follows.

1) *Visual Global and Local Perception*: As shown in Fig. 2 (a), to enhance visual comprehension, the high-resolution inputted images are divided into sub-images for local visual perception. Concurrently, the images are downsampled into lower resolutions and combined with the sub-images for subsequent mixed encoding. The Mixed Visual Encoders (MVE) are designed to encode inputted images and their variants I^i into visual representations V_{img} . To leverage the advantages of different network architectures (CNN and Vision Transformer (ViT) [54]) and integrate the local information and contextual dependencies, the semantically complementary backbones CLIP-ConvNeXt [55] and ViT self-supervised by DINOv2 [56] are employed as MVE. This visual encoding process can be formulated as

$$V_{img} = \text{Concat} (MVE (I^i)), i = 1, 2, \dots, N. \quad (1)$$

2) *Free-form Spatial-aware*: Free-form visual prompts are expected to be flexibly used to guide the model in generating appropriate responses. The shapes of visual prompts include points, boxes, circles, scribbles, etc. To meet the need for flexible interaction at any granularity, a noise augmentation method is developed. Specifically, Gaussian distribution based on the dimensions of the box prompts is sampled to simulate the free-formed shapes. The introduced noise encompasses only a portion of the ground truth or expands it. Subsequently, considering that the visual prompts exhibit varying degrees of

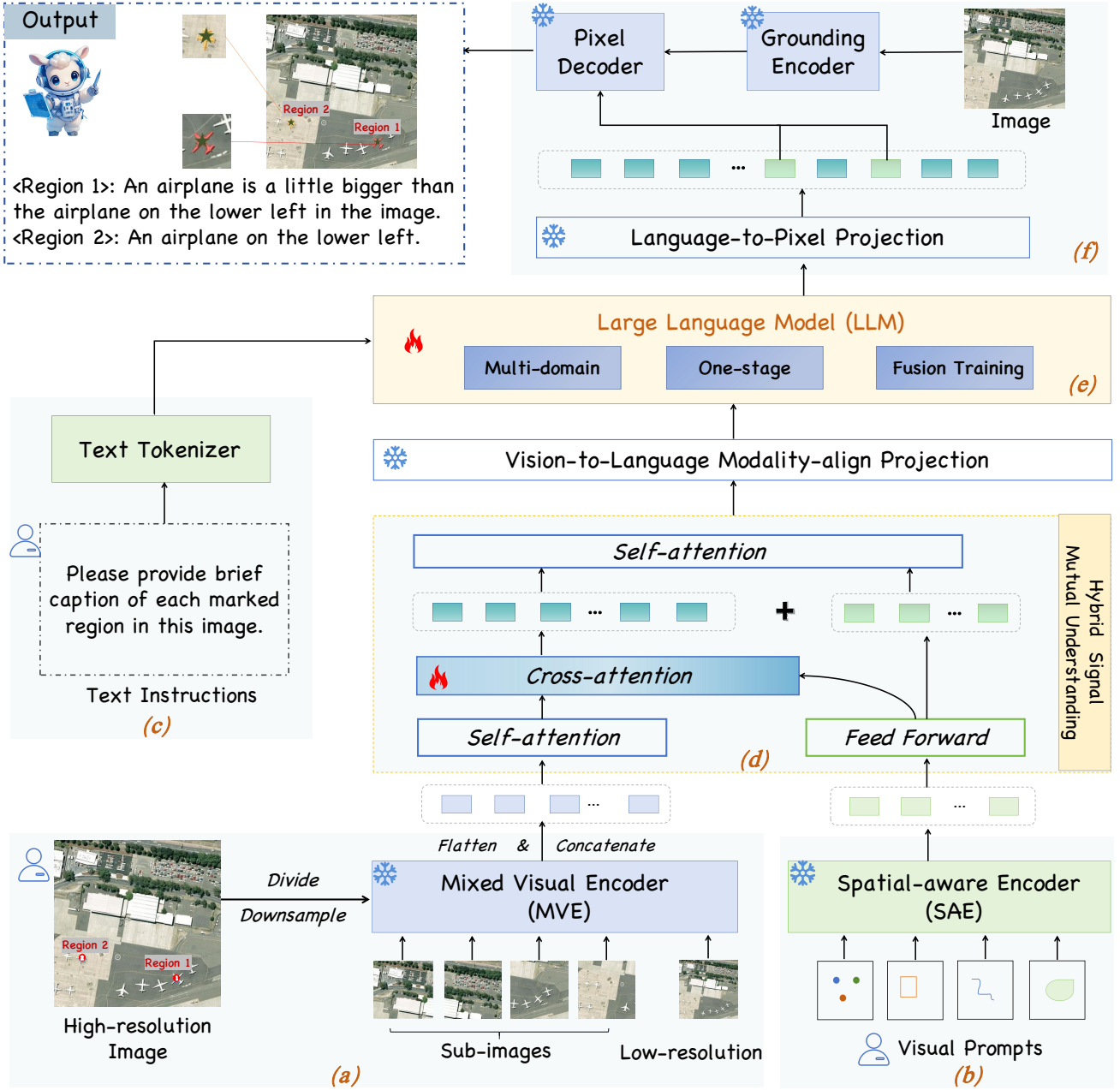


Fig. 2. Overview of the proposed EarthGPT-X model architecture.

sparsity across different shapes, as illustrated in Fig. 2 (b), a randomly initialized ViT is employed as a spatial-aware encoder (SAE) specifically for feature extraction, without any pre-trained weights suitable for image features. The various types of visual prompts V_p are encoded using the designed SAE. The implementation equation can be expressed as follows

$$E_{\text{prompt}} = \text{SAE}(V_p), \quad (2)$$

where E_{prompt} denotes the encoded visual prompts features with free-form shapes.

3) *Text Instructions Tokenizer:* As displayed in Fig. 2 (c), To facilitate linguistic comprehension, the text instructions T_{orig} are encoded by the tokenizer [57] module, and projected into language embeddings L_{instruct} , preparing for the

subsequent LLM to capture the nuanced interdependence. The detailed process after disassembly is first to use the subword tokenization [57] method to divide text instructions into subwords, enabling understanding of the structure of the linguistic signals. Subsequently, the Word2Vec [58] is adopted to map each subword to a one-dimensional vector embedding. The tokenizer process can be simply described as

$$L_{\text{instruct}} = \text{Tokenizer}(T_{\text{orig}}). \quad (3)$$

4) *Hybrid Signals Mutual Understanding:* To bridge the gap and enhance the interplay between dense visual representations and sparse visual prompts features, a hybrid signal mutual understanding mechanism is proposed. Specifically, as displayed in Fig. 2 (d), the image representations V_{img}

and visual prompts features E_{prompt} are processed by a self-attention layer and feed-forward layer to obtain V_{sa} and E_{ff} , respectively. The subsequent cross-attention and second self-attention blocks are used to compute the correlation H_{ca} between hybrid referring information and multi-scale holistic signals. In essence, this designed mechanism enhances detailed and contextual visual perception, leading to a deeper comprehension of the referring areas in holistic images. The whole procedure can be mathematically represented as

$$V_{\text{sa}} = \text{Self-attention} (V_{\text{img}}), \quad (4)$$

$$E_{\text{ff}} = \text{Feed-forward} (E_{\text{prompt}}), \quad (5)$$

$$H_{\text{ca}} = \text{Cross-attention} (V_{\text{sa}}, E_{\text{ff}}), \quad (6)$$

$$[V-P]_{\text{hybrid}} = \text{Self-attention} (V_{\text{ca}} + R_{\text{ff}}), \quad (7)$$

where $[V-P]_{\text{hybrid}}$ is the output of this designed module, containing rich visual information and spatial-aware knowledge from the free-form visual prompts. Then, the hybrid visual features are projected to the same dimension as text embeddings through the vision-to-language modality-align projection layer $\mathcal{F}_{\text{vl-p}}$. This process can be formulated as

$$[V-P]_{\text{proj}} = \mathcal{F}_{\text{vl-p}} ([V-P]_{\text{hybrid}}). \quad (8)$$

where $[V-P]_{\text{proj}}$ involve both multi-scale visual signals and free-form spatial-aware information. Notably, the cross-attention layer is updatable during the training.

B. Cross-domain One-Stage Fusion Training

The previous training pipeline of MLLM routinely uses a step-wise training strategy [8], [22]. However, in the previous pipeline, extensive manual intervention is required. For example, the researcher needs to manually set the different trainable parameters and datasets across various stages. To alleviate the need for manual efforts without sacrificing performance, the cross-domain one-stage fusion training [11] strategy is designed. Most importantly, this strategy further facilitates multi-domain (i.e., natural, optical, SAR, and infrared) data mutual understanding.

In this stage, the projected hybrid tokens are concatenated with the text instruction embeddings L_{instruct} to develop the multi-modal LLM input \mathcal{X} . Subsequently, the integrated multi-modal input is injected into LLM for alignment and deeply interactive understanding (see Fig. 2 (e)). The process can be expressed as

$$Y = \text{LLM} ([V-P]_{\text{proj}}, L_{\text{instruct}}). \quad (9)$$

Unlike other models that introduce additional learnable parameters, to simplify the model structure, the Transformer's attention layers are unfrozen during the training. Specifically, the self-attention head consists of key K , query Q , and the value V , which are implemented by linear layers. The implementations can be expressed as follows

$$Q(\mathcal{X}) = W_q \mathcal{X} + b_q, \quad (10)$$

$$K(\mathcal{X}) = W_k \mathcal{X} + b_k, \quad (11)$$

$$V(\mathcal{X}) = W_v \mathcal{X} + b_v, \quad (12)$$

where \mathcal{X} denotes multi-modal input. The parameters W_q , W_k , W_v , b_q , b_k , and b_v are updatable during the training.

To summarize, the essence of this process lies in leveraging multi-domain knowledge to generalize versatile visual reasoning ability into RS multi-source complex scenarios interpretation. Furthermore, through tuning on unified abundant visual prompt-based instruction data, the proposed EarthGPT-X can accomplish referring comprehension of RS imagery with the user's free-form visual prompts and text instruction-following.

C. Pixel Perception

To unify *referring and grounding* in one framework and achieve pixel-level grounding, the pixel encoder-decoder architecture is employed to render the referring object masks, which are shown in Fig. 2 (f). In particular, the special token pix is adopted to represent the pixel grounding masks as embeddings [59]. The embeddings L_{pix} are generated from the LLM output corresponding to the pix token. Then, the language-to-pixel projection layer $\mathcal{R}_{\text{lp-p}}$ transforms the embeddings L_{pix} into the pixel decoder's feature space. In addition, the grounding encoder is denoted as \mathcal{G} , the pixel decoder \mathcal{P} . The binary segmentation mask M generated process can be represented as follows

$$M = \mathcal{P}(\mathcal{R}_{\text{lp}}(L_{\text{pix}}), \mathcal{G}(I)). \quad (13)$$

In summary, based on the designed tripartite architecture and all-in-one training strategy, the proposed EarthGPT-X can be expected to effectively and comprehensively realize cross-modal and multi-source knowledge comprehension. Moreover, EarthGPT-X can handle multi-grained RS visual tasks, and flexibly unifies referring and grounding in one framework.

IV. DATASET CONSTRUCTION

The goal is to endow the proposed model with flexible and comprehension interpretation abilities on multi-source imagery. However, existing infrared and SAR datasets are limited to object detection tasks, hindering the development of various advanced reasoning capabilities. To address this limitation and unleash the potential of MLLMs to comprehend diverse RS data, a multi-source visual prompt-based instruction dataset named M-RSVP is constructed. Particularly, the natural and optical RS image data, which involves a wide range of visual tasks, are utilized for LLM mixed tuning. In essence, multi-domain data fusion facilitates generalizing the universal domain reasoning capabilities into limited SAR and infrared scenarios. The specific M-RSVP construction pipeline is detailed as follows.

A. Raw Data Selection

In order to develop multi-source image understanding abilities of the proposed EarthGPT-X, it is indispensable to utilize data from different scenes and sensors, including outdoor natural images, RS optical images, SAR, and infrared images, covering different visual task types. Thus, the natural scene dataset we selected is OpenImages [60] which meets this characteristic and is ideal for training the model's visual perception capabilities in general environments. Moreover, we also

choose Visual Genome [61] for training, to practice reasoning over multi-region and multi-object interactions. Meanwhile, for the RS optical dataset, we use RSVP [22] which is the first RS visual prompting dataset, allowing the model to develop region/point interpretation skills in diverse geographic and environmental settings. Furthermore, SAR detection datasets includes SSDD [62], AIR-SARShip-2.0 [63], SARDet [64], MSAR [65], and SAR-Aircraft [66]. Infrared object detection contains Sea-shipping, Infrared-security [67], Aerial-mancar [68], Double-light-vehicle [69], and HIT-UAV [70]. Leveraging multi-domain datasets is beneficial for equipping the proposed model to obtain robust generalization capabilities and to handle a wide range of visual tasks. In addition, multi-source data integration ensures comprehensive and flexible image understanding across multiple domains and sensor types.

B. Multi-source Data Unification

In specific, a unified data re-annotation method is adopted to label multi-source data. The diverse multi-source data are uniformly reorganized and relabeled as *image-visual prompts-text* triples. The regional data are based on multi-source detection datasets and ground truth bounding boxes are used as visual prompts to recognize object-level categories. Image-level tasks use the boxes $[0, 0, \text{width}, \text{height}]$, which can cover the entire image as the visual prompt. Most importantly, to support free-form visual prompts, a noise augmentation method is developed. Specifically, Gaussian distribution based on the dimensions of the box prompts is sampled to simulate the free-formed shapes. The introduced noise encompasses only a portion of the ground truth or expands it. Through restructuring public datasets formatted into unified visual prompt-based instruction following data, the structure of our training data is [“from”: “user”, “value”: “Please identify the object category of each marked region in the image.”], [“from”: “model”, “value”: “< Region1 >: Label 1\n < Region2 >: Label 2\n < Region3 >: Label 3\n.....”]. Furthermore, the GPT-4V [23] is utilized to generate more complex visual descriptions for multi-source images [22]. On top of that, by adopting the Set-of-Marks (SoM) prompting [71], we effectively leverage GPT4V’s outstanding visual reasoning capabilities to capture comprehensive and distinctive characteristics from multi-source RS data.

In conclusion, all the various datasets from different domains are combined for mixed training to deepen mutual understanding. The multiple free-form visual prompts are allowed to instruct the model to generate suitable answers, ensuring the flexibility of human-AI interaction. Furthermore, multi-domain data fusion is beneficial to realize multi-source multi-task interpretation by leveraging the diverse features and scenarios presented in supplementary image types.

V. EXPERIMENT

A. Experimental Setups

1) *Implementation Details*: The one-stage all-in-one training is conducted in this paper. We use transformer-based decoder-only Llama 2-13B [16] as the basic LLM. The pre-trained DINOv2-ViT L/14 [56] and CLIP-ConvNeXt [55]

TABLE II
RESULTS ON REFERRING OBJECT CLASSIFICATION OF EARTHGPT-X AND OTHER MULTIPLE MLLMS ON DIOR-RSVG TEST SET.

Methods	Publication Year	Formats	SS	S-IoU
<i>Vanilla MLLMs</i>				
GeoChat [9]	CVPR 2024	Coor	79.59	68.80
Sphinx [79]	Arxiv 2023	Coor	93.72	89.37
EarthGPT [8]	TGRS 2024	Coor	94.64	90.16
<i>Natural Visual Prompting MLLMs</i>				
Sphinx-V [50]	Arxiv 2024	Box	89.07	81.62
Vip-LLava-7b [80]	CVPR 2024	Box	72.56	55.94
Vip-LLava-13b [80]	CVPR 2024	Box	74.51	60.53
<i>RS Visual Prompting MLLM</i>				
EarthMarker [22]	Arxiv 2024	Point	95.96	93.49
EarthMarker [22]	Arxiv 2024	Box	98.37	97.24
EarthGPT-X(Ours)		Point	96.02	94.12
EarthGPT-X(Ours)		Box	98.60	97.83
EarthGPT-X(Ours)		Free-form	98.30	96.56

are adopted as hybrid image encoder MVE. The training image resolution is 448×448 . Subsequently, the randomly initialized ViT model is seated as the spatial-aware encoder to refine sparse features. Then, we employ a pre-trained SAM encoder and decoder [20] as the grounding encoder and pixel decoder. The image resolution required to be reshaped for the segmentation model is 1024×1024 . Furthermore, we utilize the simple MLPs as the projection layer to realize multi-modal content dimension alignment.

Throughout the training, to keep training efficiency and preserve the generalization ability of backbone models, we only unfreeze the self-attention layers of LLM and the added cross-attention module for tuning. Other modules including visual encoders, projection layers, etc., are kept frozen. The AdamW optimizer [72] with a weight decay of 0.01 and a learning rate of $2e-5$ is utilized. The total training is conducted on 8 NVIDIA A100 GPUs with 80 GB memory.

2) *Evaluation Metrics*: We adopt Semantic Intersection over Union (S-IoU) and Semantic Similarity (SS) [73] as evaluation metrics on referring object classification tasks. Furthermore, we evaluate the performance of the proposed model on the region captioning tasks based on metrics for assessing language generation quality, including BLEU [74], METEOR [75], ROUGE [76], CIDER [77], and SPICE [78]. Those metrics provide a diverse and comprehensive assessment of the quality of identified object information and generated region captions.

B. Referring Object Classification

To assess the merits of the proposed EarthGPT-X, we report its performance and compare it with the recent vanilla MLLMs and visual prompting MLLMs on DIOR-RSVG [7]. For referring object classification tasks, the text instruction is

TABLE III
RESULTS ON REGION CAPTIONING OF EARTHGPT-X AND OTHER MLLMs ON THE OPT-RSVG TEST SET.

Method	Publication Year	Format	BLEU-1	BLEU-2	BLEU-3	BLEU-4	METEOR	ROUGE	CIDER	SPICE
<i>Vanilla MLLMs</i>										
Qwen-VL-Chat [9]	Arxiv 2023	Coor	12.78	6.47	2.77	1.24	5.97	17.06	13.15	6.60
GeoChat [81]	CVPR 2024	Coor	15.02	8.49	5.21	3.29	9.24	25.65	42.86	16.10
Sphinx [79]	Arxiv 2023	Coor	22.79	15.27	10.97	7.84	12.95	30.28	105.85	20.18
EarthGPT [8]	TGRS 2024	Coor	30.28	19.99	13.58	8.73	15.29	31.52	88.92	21.05
<i>Visual Prompting MLLMs</i>										
Sphinx-V [50]	Arxiv 2024	Box	23.35	14.84	10.37	7.16	14.10	32.08	81.79	22.46
Vip-LLava-7b [80]	CVPR 2024	Box	14.67	7.29	4.06	2.25	8.20	20.17	23.47	12.79
Vip-LLava-13b [80]	CVPR 2024	Box	16.39	8.40	4.77	2.80	8.47	21.36	25.85	12.41
GLaMM [80]	CVPR 2024	Box	12.50	6.06	3.25	1.74	7.98	22.01	23.85	12.40
EarthGPT-X(Ours)		Point	52.22	48.13	45.15	42.88	35.01	64.31	477.40	63.14
EarthGPT-X(Ours)		Box	64.55	59.76	56.10	53.11	39.22	66.64	487.44	64.20
EarthGPT-X(Ours)		Free-form	63.25	58.16	54.89	52.01	38.35	65.01	482.26	63.23

“Please identify the object category of the marked region in the image”. The vanilla MLLMs do not support drawing visual prompts on the images, therefore, the coordinates contained in the text instruction serve as the referring regions. The vanilla MLLMs including natural MLLMs Sphinx [79], RS MLLMs GeoChat [81], and EarthGPT [8]. We select the most recent natural visual prompting MLLMs including Sphinx-V [50], Vip-LLava [80], and the RS visual prompting MLLM model EarthMarker [22] as the comparison.

As shown in Tab. II, EarthGPT-X achieves 98.40 % in SS and 97.13 % in S-IoU under box prompts. We also observe that the box-level results are better than the point and free-form prompts ones. This experiment shows that our model achieves remarkable referring object classification performances compared with other vanilla MLLMs, natural and RS visual prompting MLLMs. Furthermore, we also conduct qualitative analysis to provide an intuitive performance display of EarthGPT-X. As illustrated in Fig. 3, the infrared image showcases a residential leisure area, and for the three marked regions, all other MLLMs respond incorrectly. Conversely, EarthGPT-X successfully recognizes the human, vehicle, and basketball court targets. Following this is a fuzzy port SAR image, where it is difficult to visually distinguish between ships and storage tanks. EarthGPT-X delivers precise interpretations for these targets, whereas other models perform poorly, except for EarthGPT. These results prove the significance of our work that empowers the MLLMs with fine-grained reasoning ability for multi-source object-level comprehension.

C. Region Captioning

For the brief region captioning, the test set of OPT-RSVG [82] is employed for zero-shot evaluation. We elaborately choose both natural and RS-specific MLLMs for performance comparison. Natural scene MLLMs contains Qwen-VL-Chat [9], Sphinx [79], Sphinx-V [50], Vip-LLava [80] and GLaMM [80]. Popular RS-specific MLLMs GeoChat [81] and EarthGPT [8] are selected. The text instruction for the region captioning task is designed as “Please provide a brief caption

of each marked region in the image”. As displayed in Tab. III, the proposed EarthGPT-X significantly outperforms the previous works on all of the evaluation metrics. Notably, using boxes as visual prompts can yield the best performance on region captioning and dialogue ability.

D. Comprehensive Capabilities Evaluation

Traditional vision models in the RS field primarily focus on a single visual modality and single tasks, exhibiting poor generalization [83]–[85]. Thanks to our M-RSVP’s rich multi-sensor knowledge, EarthGPT-X has robust generalization capabilities across optical, SAR, and infrared visual modalities. To verify and assess the comprehensive capabilities of the proposed model, we conduct a thorough qualitative evaluation. Our assessment also covers multi-source images and multiple levels of image interpretation granularity, including image, point, box, and free-form prompted levels. Moreover, the evaluated visual tasks are extensive, such as brief captioning, detailed captioning, ground captioning, region captioning, referring object classification, and inter-relationship analyses. As displayed in Fig. 4, our model demonstrates remarkable visual reasoning and analytical abilities. EarthGPT-X can provide detailed descriptions for multi-source images, as shown in the interpretation results of the first image, which includes overall image depiction, number of targets, target orientation, and scene reasoning. Notably, in the relationship analysis of the second and third images, EarthGPT-X provides detailed and comprehensive responses. Specifically, EarthGPT-X adeptly summarizes the connections between various regions and the overall image relationship, and then analyzes the characteristics and attributes of the targets within each specific area. In summary, EarthGPT-X demonstrates a profound ability to dissect and understand complex visual information in the multi-source RS MLLMs.

E. Pixel Grounding

To evaluate the pixel grounding capabilities of the proposed model, we specifically chose images that feature complex and

User Input:

- Text Instruction: *Please identify the object category of each marked region in the image.*
- A Infrared Image and three marked regions:

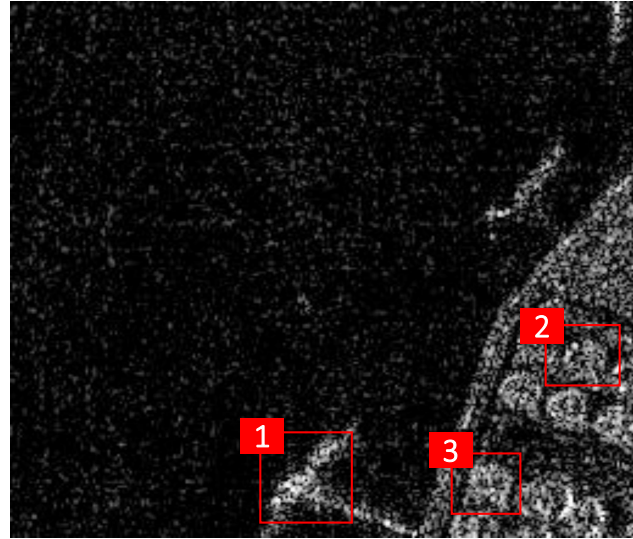


Model Response:

<p>EarthGPT-X </p> <p><Region 1>: Vehicle. <Region 2>: Person. <Region 3>: Basketball court.</p>	<p>Sphinx-V </p> <p><Region 1>: Compact car. <Region 2>: Person. <Region 3>: House.</p>
<p>GeoChat </p> <p><Region 1>: Large-vehicle. <Region 2>: Bridge. <Region 3>: Buildings.</p>	<p>EarthGPT </p> <p><Region 1>: People. <Region 2>: People. <Region 3>: Golf field.</p>
<p>Sphinx </p> <p><Region 1><Region 2>< Region 3>: No visible labels.</p>	<p>Vip-LLava-13b </p> <p><Region 1>: Car. <Region 2>: Person. <Region 3>: Parking lot.</p>

User Input:

- Text Instruction: *Please identify the object category of each marked region in the image.*
- A SAR Image and three marked regions:



Model Response:

<p>EarthGPT-X </p> <p><Region 1>: Ship. <Region 2>: Storage_tank. <Region 3>: Storage_tank</p>	<p>Sphinx-V </p> <p><Region 1>: Bridge. <Region 2>: Ship. <Region 3>: Ship.</p>
<p>GeoChat </p> <p><Region 1>: Harbor. <Region 2>: Ship. <Region 3>: Ship.</p>	<p>EarthGPT </p> <p><Region 1>: Ship. <Region 2>: Tank. <Region 3>: Tank.</p>
<p>Sphinx </p> <p><Region 1>: Ship. <Region 2>: Ship. <Region 3>: Ship.</p>	<p>Vip-LLava-13b </p> <p><Region 1>: Brige. <Region 2>: Ship. <Region 3>: Airplane.</p>

Fig. 3. The referring object classification results on multi-source RS images demonstrate the superior region-level RS visual understanding capability of EarthGPT-X, compared to other vanilla and visual prompting MLLMs (the black text indicates consistency with the ground truth, the red text represents incorrect answers).

different scenes with multiple targets. This experiment aims to test the model’s robustness and precision in identifying and segmenting diverse elements within a single frame. As shown in Fig. 5, the first test image is the port scene, we mark a ship and a tiny vehicle to assess the model’s ability to discern and accurately interpret tiny targets amidst a busy background. Surprisingly, EarthGPT-X not only recognized these smaller objects but also effectively segmented them from the surrounding environment. Another test involved an image from an urban sports center where we marked five distinct targets scattered across different areas, including varied elements such as a swimming pool, tennis court, vehicle, etc. This scenario tests the model’s capacity to handle spatially separated objects

within a complex urban setting. EarthGPT-X demonstrates exceptional performances in precise object recognition and pixel-grounding. Moreover, these tests highlight EarthGPT-X’s advanced pixel understanding capabilities and its potential to enhance RS image analyses across different visual modalities.

F. Ablation Study

In this section, we analyze the impact of key components of EarthGPT-X in detail.

1) *Different Visual Encoders*: To show the effectiveness of the proposed hybrid MVE module, we ablate on the performance of our EarthGPT-X when using different visual encoders. Specifically, this ablation uses CLIP-ConvNeXt-L,



Fig. 4. Example visualization of EarthGPT-X for multi-source (optical, SAR, and infrared) image comprehension and multiple visual tasks reasoning under various visual prompts.

CLIP RN50×16, and DINOv2 ViT-L/14 for comparison. The results are shown in Tab. IV, it is clear that the setting using the ConvNeXt-L and DINOv2 ViT-L/14 as the mixed visual experts achieve the most superior performance. The performance of both SS and S-IoU increases accordingly. These results demonstrate that utilizing a network architecture with complementary functions has deepened the understanding of local information and contextual dependencies on RS imagery.

2) *Sub-images Decomposition and Multi-scale:* In the visual feature extraction phase of our approach, we enhance the integration of visual features by incorporating multiple scales

and high-resolution sub-images, enabling a more profound comprehension of RS images. To evaluate the effectiveness of our modified feature extraction strategy, we conduct ablation studies focusing on the impact of multi-scale features and high-resolution sub-images on the performance of our EarthGPT-X model. As shown in Tab. V, utilizing the multi-scale and sub-images features setting achieves superior performance over single-scale features. These results demonstrate that the detailed analysis of these high-resolution sub-images and more scales allows for capturing finer details that are crucial for accurate interpretation and analysis.

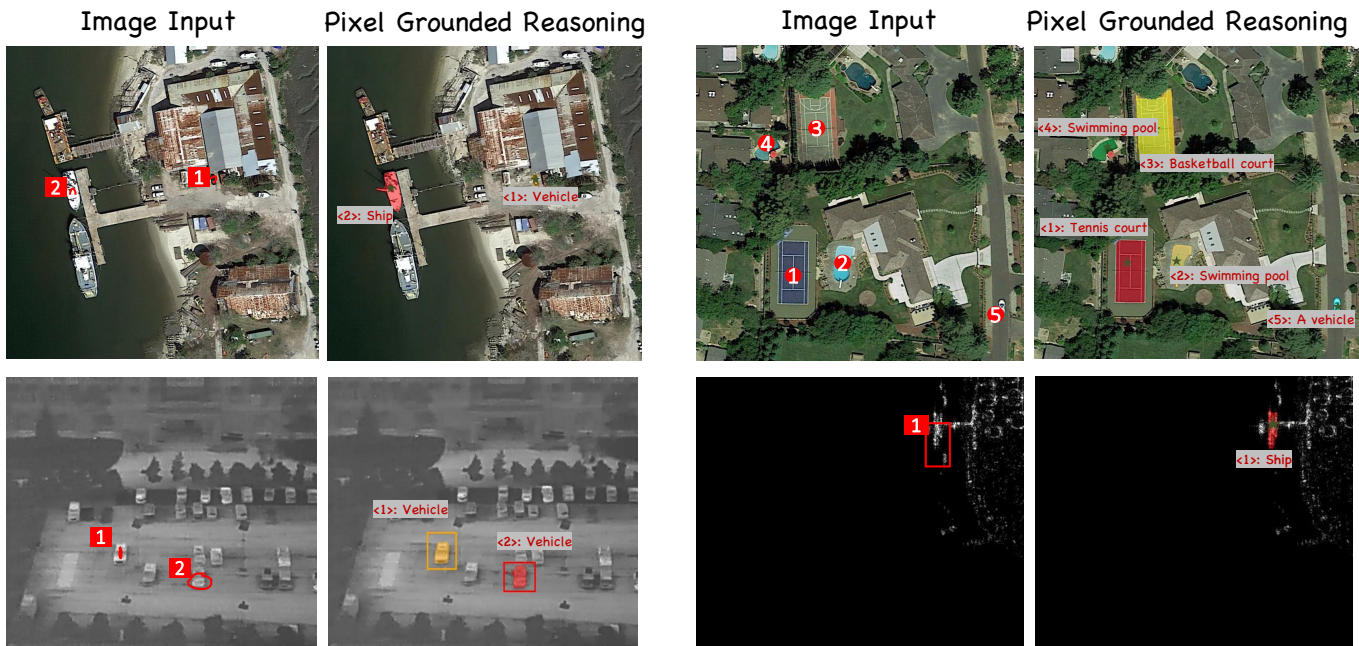


Fig. 5. Pixel grounding examples of EarthGPT-X on multi-source imagery (EarthGPT-X’s interpretation of the object classes is also displayed on the figures).

TABLE IV
ABLATION RESULTS ON DIFFERENT VISUAL ENCODERS.

CLIP	CLIP	DINOv2	SS	S-IoU
ConvNeXt-L	RN50×16	ViT-L/14		
✓	✗	✗	96.73	95.82
✗	✓	✗	95.28	94.17
✗	✗	✓	94.51	94.01
✗	✓	✓	97.68	96.67
✓	✗	✓	98.40	97.13

TABLE V
ABLATION RESULTS ON IMAGE PRE-PROCESSING.

Settings	Visual Encoder	SS	S-IoU
Single-scale	MVE	94.93	95.05
Multi-scale	MVE	96.18	95.29
Multi-scale + Sub-images	MVE	98.40	97.13

VI. CONCLUSION

In this paper, we propose EarthGPT-X, a flexible and versatile MLLM specifically designed for understanding RS imagery from multiple sources. As the first RS spatial model to unify *referring and grounding* tasks within a visual prompting framework, EarthGPT-X represents a significant advancement in the application of MLLMs to the RS domain. Technically, the hybrid signal mutual understanding mechanism is developed to enhance the interplay between dense visual features, sparse free-form visual prompts, and text instructions, facilitating a multi-grained understanding of complex RS imagery.

Furthermore, a novel cross-domain one-stage fusion training strategy is proposed to generalize general-domain knowledge into RS multi-source scenarios, such as SAR and infrared. Through the designed visual prompt learning framework and training strategy, EarthGPT-X achieves multi-grained visual understanding at the image, region, pixel levels, etc., allowing for precise and intelligent analyses in real-world applications. In the future, we plan to enrich the SAR and infrared datasets to encompass a broader range of tasks, addressing the current limitation of narrow scope. Additionally, we aim to enable EarthGPT-X to perform more complex visual reasoning tasks across multiple visual modalities, further solidifying EarthGPT-X as a versatile and powerful tool for comprehensive RS imagery analyses.

REFERENCES

- [1] Haoxuan You, Haotian Zhang, Zhe Gan, Xianzhi Du, Bowen Zhang, Zirui Wang, Liangliang Cao, Shih-Fu Chang, and Yinfei Yang. Ferret: Refer and ground anything anywhere at any granularity. *arXiv preprint arXiv:2310.07704*, 2023.
- [2] Yang Zhan, Zhitong Xiong, and Yuan Yuan. Rsvg: Exploring data and models for visual grounding on remote sensing data. *IEEE Transactions on Geoscience and Remote Sensing*, 61:1–13, 2023.
- [3] Yuqian Yuan, Wentong Li, Jian Liu, Dongqi Tang, Xinjie Luo, Chi Qin, Lei Zhang, and Jianke Zhu. Osprey: Pixel understanding with visual instruction tuning. *arXiv preprint arXiv:2312.10032*, 2023.
- [4] Shilong Zhang, Peize Sun, Shoufa Chen, Min Xiao, Wenqi Shao, Wenwei Zhang, Kai Chen, and Ping Luo. Gpt4roi: Instruction tuning large language model on region-of-interest. *arXiv preprint arXiv:2307.03601*, 2023.
- [5] Qiang Zhou, Chaohui Yu, Shaofeng Zhang, Sitong Wu, Zhibing Wang, and Fan Wang. Regionblip: A unified multi-modal pre-training framework for holistic and regional comprehension. *arXiv preprint arXiv:2308.02299*, 2023.
- [6] Keqin Chen, Zhao Zhang, Weili Zeng, Richong Zhang, Feng Zhu, and Rui Zhao. Shikra: Unleashing multimodal llm’s referential dialogue magic. *arXiv preprint arXiv:2306.15195*, 2023.
- [7] Yang Zhan, Zhitong Xiong, and Yuan Yuan. Rsvg: Exploring data and models for visual grounding on remote sensing data. *IEEE Transactions on Geoscience and Remote Sensing*, 61:1–13, 2023.

- [8] Wei Zhang, Miaoxin Cai, Tong Zhang, Yin Zhuang, and Xuerui Mao. Earthgpt: A universal multi-modal large language model for multi-sensor image comprehension in remote sensing domain. *IEEE Transactions on Geoscience and Remote Sensing*, 2024.
- [9] Kartik Kuckreja, Muhammad Sohail Danish, Muzammal Naseer, Abhijit Das, Salman Khan, and Fahad Shahbaz Khan. Geochat: Grounded large vision-language model for remote sensing. In *Proceedings of the IEEE/CVF Conference on Computer Vision and Pattern Recognition*, pages 27831–27840, 2024.
- [10] Rowan Zellers, Yonatan Bisk, Ali Farhadi, and Yejin Choi. From recognition to cognition: Visual commonsense reasoning. In *Proceedings of the IEEE/CVF conference on computer vision and pattern recognition*, pages 6720–6731, 2019.
- [11] Peng Gao, Renrui Zhang, Chris Liu, Longtian Qiu, Siyuan Huang, Weifeng Lin, Shitian Zhao, Shijie Geng, Ziyi Lin, Peng Jin, et al. Sphinx-x: Scaling data and parameters for a family of multi-modal large language models. *arXiv preprint arXiv:2402.05935*, 2024.
- [12] Tom Brown, Benjamin Mann, Nick Ryder, Melanie Subbiah, Jared D Kaplan, Prafulla Dhariwal, Arvind Neelakantan, Pranav Shyam, Girish Sastry, Amanda Askell, et al. Language models are few-shot learners. *Advances in neural information processing systems*, 33:1877–1901, 2020.
- [13] OpenAI. Chatgpt. <https://chat.openai.com>, 2023a.
- [14] OpenAI. Gpt-4 technical report, 2023.
- [15] Hugo Touvron, Thibaut Lavril, Gautier Izacard, Xavier Martinet, Marie-Anne Lachaux, Timothée Lacroix, Baptiste Rozière, Naman Goyal, Eric Hambro, Faisal Azhar, et al. Llama: Open and efficient foundation language models. *arXiv preprint arXiv:2302.13971*, 2023a.
- [16] Hugo Touvron, Louis Martin, Kevin Stone, Peter Albert, Amjad Almahairi, Yasmine Babaei, Nikolay Bashlykov, Soumya Batra, Prajjwal Bhargava, Shruiti Bhosale, et al. Llama 2: Open foundation and fine-tuned chat models. *arXiv preprint arXiv:2307.09288*, 2023b.
- [17] Peng Gao, Jiaming Han, Renrui Zhang, Ziyi Lin, Shijie Geng, Aojun Zhou, Wei Zhang, Pan Lu, Conghui He, Xiangyu Yue, et al. Llama-adapter v2: Parameter-efficient visual instruction model. *arXiv preprint arXiv:2304.15010*, 2023.
- [18] Renrui Zhang, Jiaming Han, Aojun Zhou, Xiangfei Hu, Shilin Yan, Pan Lu, Hongsheng Li, Peng Gao, and Yu Qiao. Llama-adapter: Efficient fine-tuning of language models with zero-init attention. *arXiv preprint arXiv:2303.16199*, 2023.
- [19] Menglin Jia, Luming Tang, Bor-Chun Chen, Claire Cardie, Serge Belongie, Bharath Hariharan, and Ser-Nam Lim. Visual prompt tuning. In *European Conference on Computer Vision*, pages 709–727. Springer, 2022.
- [20] Alexander Kirillov, Eric Mintun, Nikhila Ravi, Hanzi Mao, Chloe Rolland, Laura Gustafson, Tete Xiao, Spencer Whitehead, Alexander C Berg, Wan-Yen Lo, et al. Segment anything. In *Proceedings of the IEEE/CVF International Conference on Computer Vision*, pages 4015–4026, 2023.
- [21] Keyan Chen, Chenyang Liu, Hao Chen, Haotian Zhang, Wenyuan Li, Zhengxia Zou, and Zhenwei Shi. Rsprompter: Learning to prompt for remote sensing instance segmentation based on visual foundation model. *IEEE Transactions on Geoscience and Remote Sensing*, 2024.
- [22] Wei Zhang, Miaoxin Cai, Tong Zhang, Yin Zhuang, and Xuerui Mao. Earthmarker: A visual prompt learning framework for region-level and point-level remote sensing imagery comprehension. *arXiv preprint arXiv:2407.13596*, 2024.
- [23] Josh Achiam, Steven Adler, Sandhini Agarwal, Lama Ahmad, Ilge Akkaya, Florencia Leoni Aleman, Diogo Almeida, Janko Altmenschmidt, Sam Altman, Shyamal Anadkat, et al. Gpt-4 technical report. *arXiv preprint arXiv:2303.08774*, 2023.
- [24] Long Ouyang, Jeffrey Wu, Xu Jiang, Diogo Almeida, Carroll Wainwright, Pamela Mishkin, Chong Zhang, Sandhini Agarwal, Katarina Slama, Alex Ray, et al. Training language models to follow instructions with human feedback. *Advances in Neural Information Processing Systems*, 35:27730–27744, 2022.
- [25] Hugo Touvron, Thibaut Lavril, Gautier Izacard, Xavier Martinet, Marie-Anne Lachaux, Timothée Lacroix, Baptiste Rozière, Naman Goyal, Eric Hambro, Faisal Azhar, et al. Llama: Open and efficient foundation language models. *arXiv preprint arXiv:2302.13971*, 2023.
- [26] Rohan Taori, Ishaan Gulrajani, Tianyi Zhang, Yann Dubois, Xuechen Li, Carlos Guestrin, Percy Liang, and Tatsunori B Hashimoto. Alpaca: A strong, replicable instruction-following model. *Stanford Center for Research on Foundation Models*. <https://crfm.stanford.edu/2023/03/13/alpaca.html>, 3(6):7, 2023.
- [27] Wei-Lin Chiang, Zhuohan Li, Zi Lin, Ying Sheng, Zhanghao Wu, Hao Zhang, Lianmin Zheng, Siyuan Zhuang, Yonghao Zhuang, Joseph E Gonzalez, et al. Vicuna: An open-source chatbot impressing gpt-4 with 90%* chatgpt quality. See <https://vicuna.lmsys.org> (accessed 14 April 2023), 2023.
- [28] Baolin Peng, Chunyuan Li, Pengcheng He, Michel Galley, and Jianfeng Gao. Instruction tuning with gpt-4. *arXiv preprint arXiv:2304.03277*, 2023.
- [29] Jun Chen, Han Guo, Kai Yi, Boyang Li, and Mohamed Elhoseiny. Visualgpt: Data-efficient adaptation of pretrained language models for image captioning. In *Proceedings of the IEEE/CVF Conference on Computer Vision and Pattern Recognition*, pages 18030–18040, 2022.
- [30] Junnan Li, Dongxu Li, Silvio Savarese, and Steven Hoi. Blip-2: Bootstrapping language-image pre-training with frozen image encoders and large language models. *arXiv preprint arXiv:2301.12597*, 2023.
- [31] Haotian Liu, Chunyuan Li, Qingyang Wu, and Yong Jae Lee. Visual instruction tuning. *arXiv preprint arXiv:2304.08485*, 2023.
- [32] Jean-Baptiste Alayrac, Jeff Donahue, Pauline Luc, Antoine Miech, Iain Barr, Yana Hasson, Karel Lenc, Arthur Mensch, Katherine Millican, Malcolm Reynolds, et al. Flamingo: a visual language model for few-shot learning. *Advances in Neural Information Processing Systems*, 35:23716–23736, 2022.
- [33] Shaohan Huang, Li Dong, Wenhui Wang, Yaru Hao, Saksham Singhal, Shuming Ma, Tengchao Lv, Lei Cui, Owais Khan Mohammed, Qiang Liu, et al. Language is not all you need: Aligning perception with language models. *arXiv preprint arXiv:2302.14045*, 2023.
- [34] Deyao Zhu, Jun Chen, Xiaoqian Shen, Xiang Li, and Mohamed Elhoseiny. Minigt-4: Enhancing vision-language understanding with advanced large language models. *arXiv preprint arXiv:2304.10592*, 2023.
- [35] Qinghao Ye, Haiyang Xu, Guohai Xu, Jiabo Ye, Ming Yan, Yiyang Zhou, Junyang Wang, Anwen Hu, Pengcheng Shi, Yaya Shi, et al. mplug-owl: Modularization empowers large language models with multimodality. *arXiv preprint arXiv:2304.14178*, 2023.
- [36] Chenyang Lyu, Minghao Wu, Longyue Wang, Xinting Huang, Bingshuai Liu, Zefeng Du, Shuming Shi, and Zhaopeng Tu. Macaw-llm: Multi-modal language modeling with image, audio, video, and text integration. *arXiv preprint arXiv:2306.09093*, 2023.
- [37] Zineng Tang, Ziyi Yang, Mahmoud Khademi, Yang Liu, Chenguang Zhou, and Mohit Bansal. Codi-2: In-context, interleaved, and interactive any-to-any generation. *arXiv preprint arXiv:2311.18775*, 2023.
- [38] Runsen Xu, Xiaolong Wang, Tai Wang, Yilun Chen, Jiangmiao Pang, and Dahua Lin. Pointllm: Empowering large language models to understand point clouds. *arXiv preprint arXiv:2308.16911*, 2023.
- [39] Ziyu Guo, Renrui Zhang, Xiangyang Zhu, Yiwen Tang, Xianzheng Ma, Jiaming Han, Kexin Chen, Peng Gao, Xianzhi Li, Hongsheng Li, et al. Point-bind & point-llm: Aligning point cloud with multi-modality for 3d understanding, generation, and instruction following. *arXiv preprint arXiv:2309.00615*, 2023.
- [40] Yining Hong, Haoyu Zhen, Peihao Chen, Shuhong Zheng, Yilun Du, Zhenfang Chen, and Chuang Gan. 3d-llm: Injecting the 3d world into large language models. *arXiv preprint arXiv:2307.12981*, 2023.
- [41] Yuan Hu, Jianlong Yuan, Congcong Wen, Xiaonan Lu, and Xiang Li. Rsgpt: A remote sensing vision language model and benchmark. *arXiv preprint arXiv:2307.15266*, 2023.
- [42] Wenliang Dai, Junnan Li, Dongxu Li, Anthony Meng Hua Tong, Junqi Zhao, Weisheng Wang, Boyang Li, Pascale Fung, and Steven Hoi. Instructblip: Towards general-purpose vision-language models with instruction tuning, 2023.
- [43] Dilxat Muhtar, Zhenshi Li, Feng Gu, Xueliang Zhang, and Pengfeng Xiao. Lhrs-bot: Empowering remote sensing with vgi-enhanced large multimodal language model. *arXiv preprint arXiv:2402.02544*, 2024.
- [44] Taylor Shin, Yasaman Razeghi, Robert L Logan IV, Eric Wallace, and Sameer Singh. Autoprompt: Eliciting knowledge from language models with automatically generated prompts. *arXiv preprint arXiv:2010.15980*, 2020.
- [45] Kaiyang Zhou, Jingkang Yang, Chen Change Loy, and Ziwei Liu. Learning to prompt for vision-language models. *International Journal of Computer Vision*, 130(9):2337–2348, 2022.
- [46] Yu Du, Fangyun Wei, Ziheng Zhang, Miaojing Shi, Yue Gao, and Guoqi Li. Learning to prompt for open-vocabulary object detection with vision-language model. In *Proceedings of the IEEE/CVF Conference on Computer Vision and Pattern Recognition*, pages 14084–14093, 2022.
- [47] Chengjian Feng, Yujie Zhong, Zequn Jie, Xiangxiang Chu, Haibing Ren, Xiaolin Wei, Weidi Xie, and Lin Ma. Promptdet: Towards open-vocabulary detection using uncurated images. In *European Conference on Computer Vision*, pages 701–717. Springer, 2022.
- [48] Feng Li, Hao Zhang, Peize Sun, Xueyan Zou, Shilong Liu, Jianwei Yang, Chunyuan Li, Lei Zhang, and Jianfeng Gao. Semantic-sam: Segment and

- recognize anything at any granularity. *arXiv preprint arXiv:2307.04767*, 2023.
- [49] Yuan Yao, Ao Zhang, Zhengyan Zhang, Zhiyuan Liu, Tat-Seng Chua, and Maosong Sun. Cpt: Colorful prompt tuning for pre-trained vision-language models, 2022.
- [50] Weifeng Lin, Xinyu Wei, Ruichuan An, Peng Gao, Bocheng Zou, Yulin Luo, Siyuan Huang, Shanghang Zhang, and Hongsheng Li. Draw-and-understand: Leveraging visual prompts to enable mlms to comprehend what you want. *arXiv preprint arXiv:2403.20271*, 2024.
- [51] Yakoub Bazi, Laila Bashmal, Mohamad Mahmoud Al Rahhal, Riccardo Ricci, and Farid Melgani. Rs-llava: A large vision-language model for joint captioning and question answering in remote sensing imagery. *Remote Sensing*, 16(9):1477, 2024.
- [52] Wei Zhang, Miaoxin Cai, Tong Zhang, Guoqiang Lei, Yin Zhuang, and Xuerui Mao. Popeye: A unified visual-language model for multi-source ship detection from remote sensing imagery. *IEEE Journal of Selected Topics in Applied Earth Observations and Remote Sensing*, 2024. early access.
- [53] Yang Zhan, Zhitong Xiong, and Yuan Yuan. Skyeyegpt: Unifying remote sensing vision-language tasks via instruction tuning with large language model. *arXiv preprint arXiv:2401.09712*, 2024.
- [54] Alexey Dosovitskiy, Lucas Beyer, Alexander Kolesnikov, Dirk Weissenborn, Xiaohua Zhai, Thomas Unterthiner, Mostafa Dehghani, Matthias Minderer, Georg Heigold, Sylvain Gelly, Jakob Uszkoreit, and Neil Houlsby. An image is worth 16x16 words: Transformers for image recognition at scale, 2021.
- [55] Alec Radford, Jong Wook Kim, Chris Hallacy, Aditya Ramesh, Gabriel Goh, Sandhini Agarwal, Girish Sastry, Amanda Askell, Pamela Mishkin, Jack Clark, et al. Learning transferable visual models from natural language supervision. In *International conference on machine learning*, pages 8748–8763. PMLR, 2021.
- [56] Maxime Oquab, Timothée Darcet, Théo Moutakanni, Huy Vo, Marc Szafraniec, Vasil Khalidov, Pierre Fernandez, Daniel Haziza, Francisco Massa, Alaaeldin El-Nouby, et al. Dinov2: Learning robust visual features without supervision. *arXiv preprint arXiv:2304.07193*, 2023.
- [57] Taku Kudo and John Richardson. Sentencepiece: A simple and language independent subword tokenizer and detokenizer for neural text processing. *arXiv preprint arXiv:1808.06226*, 2018.
- [58] Tomas Mikolov, Kai Chen, Greg Corrado, and Jeffrey Dean. Efficient estimation of word representations in vector space. *arXiv preprint arXiv:1301.3781*, 2013.
- [59] Junwen He, Yifan Wang, Lijun Wang, Huchuan Lu, Jun-Yan He, Jin-Peng Lan, Bin Luo, and Xuansong Xie. Multi-modal instruction tuned llms with fine-grained visual perception. In *Proceedings of the IEEE/CVF Conference on Computer Vision and Pattern Recognition*, pages 13980–13990, 2024.
- [60] Alina Kuznetsova, Hassan Rom, Neil Alldrin, Jasper Uijlings, Ivan Krasin, Jordi Pont-Tuset, Shahab Kamali, Stefan Popov, Matteo Mallocci, Alexander Kolesnikov, et al. The open images dataset v4: Unified image classification, object detection, and visual relationship detection at scale. *International journal of computer vision*, 128(7):1956–1981, 2020.
- [61] Ranjay Krishna, Yuke Zhu, Oliver Groth, Justin Johnson, Kenji Hata, Joshua Kravitz, Stephanie Chen, Yannis Kalantidis, Li-Jia Li, David A Shamma, et al. Visual genome: Connecting language and vision using crowdsourced dense image annotations. *International journal of computer vision*, 123:32–73, 2017.
- [62] Tianwen Zhang, Xiaoling Zhang, Jianwei Li, Xiaowo Xu, Baoyou Wang, Xu Zhan, Yanqin Xu, Xiao Ke, Tianjiao Zeng, Hao Su, et al. Sar ship detection dataset (ssdd): Official release and comprehensive data analysis. *Remote Sensing*, 13(18):3690, 2021.
- [63] SUN Xian, WANG Zhirui, SUN Yuanrui, DIAO Wenhui, ZHANG Yue, and FU Kun. Air-sarship-1.0: High-resolution sar ship detection dataset. *Journal of Radars*, 8(6):852–863, 2019.
- [64] Yuxuan Li, Xiang Li, Weijie Li, Qibin Hou, Li Liu, Ming-Ming Cheng, and Jian Yang. Sardet-100k: Towards open-source benchmark and toolkit for large-scale sar object detection. *arXiv preprint arXiv:2403.06534*, 2024.
- [65] J Chen, Z Huang, R Xia, B Wu, L Sheng, L Sun, and B Yao. Large-scale multi-class sar image target detection dataset-1.0. *j. radars* 2022.
- [66] Wang Zhirui, Kang Yuzhuo, Zeng Xuan, WANG Yuelei, ZHANG Ting, and SUN Xian. Sar-aircraft-1.0: High-resolution sar aircraft detection and recognition dataset. *Journal of Radars*, 12(4):906–922, 2023.
- [67] InfiRay. Infrared-security. http://openai.iraytek.com/apply/Infrared_security.html/, 2021.
- [68] InfiRay. Aerial-mancar. http://openai.raytrontek.com/apply/Aerial_mancar.html/, 2021.
- [69] InfiRay. Double-light-vehicle. http://openai.raytrontek.com/apply/Double_light_vehicle.html/, 2021.
- [70] Jiashun Suo, Tianyi Wang, Xingzhou Zhang, Haiyang Chen, Wei Zhou, and Weisong Shi. Hit-uav: A high-altitude infrared thermal dataset for unmanned aerial vehicle-based object detection. *Scientific Data*, 10(1):227, 2023.
- [71] Jianwei Yang et al. Set-of-mark prompting unleashes extraordinary visual grounding in gpt-4v. *arXiv preprint arXiv:2310.11441*, 2023.
- [72] Diederik P Kingma and Jimmy Ba. Adam: A method for stochastic optimization. *arXiv preprint arXiv:1412.6980*, 2014.
- [73] Hamid Rezaatoughi, Nathan Tsoi, JunYoung Gwak, Amir Sadeghian, Ian Reid, and Silvio Savarese. Generalized intersection over union: A metric and a loss for bounding box regression. In *Proceedings of the IEEE/CVF conference on computer vision and pattern recognition*, pages 658–666, 2019.
- [74] Kishore Papineni, Salim Roukos, Todd Ward, and Wei-Jing Zhu. Bleu: a method for automatic evaluation of machine translation. In *Proceedings of the 40th annual meeting of the Association for Computational Linguistics*, pages 311–318, 2002.
- [75] Satantjeet Banerjee and Alon Lavie. Meteor: An automatic metric for mt evaluation with improved correlation with human judgments. In *Proceedings of the acl workshop on intrinsic and extrinsic evaluation measures for machine translation and/or summarization*, pages 65–72, 2005.
- [76] Chin-Yew Lin. Rouge: A package for automatic evaluation of summaries. In *Text summarization branches out*, pages 74–81, 2004.
- [77] Ramakrishna Vedantam, C Lawrence Zitnick, and Devi Parikh. Cider: Consensus-based image description evaluation. In *Proceedings of the IEEE conference on computer vision and pattern recognition*, pages 4566–4575, 2015.
- [78] Peter Anderson, Basura Fernando, Mark Johnson, and Stephen Gould. Spice: Semantic propositional image caption evaluation. In *Computer Vision—ECCV 2016: 14th European Conference, Amsterdam, The Netherlands, October 11–14, 2016, Proceedings, Part V 14*, pages 382–398. Springer, 2016.
- [79] Ziyi Lin, Chris Liu, Renrui Zhang, Peng Gao, Longtian Qiu, Han Xiao, Han Qiu, Chen Lin, Wenqi Shao, Keqin Chen, et al. Sphinx: The joint mixing of weights, tasks, and visual embeddings for multi-modal large language models. *arXiv preprint arXiv:2311.07575*, 2023.
- [80] Mu Cai, Haotian Liu, Siva Karthik Mustikovela, Gregory P Meyer, Yuning Chai, Dennis Park, and Yong Jae Lee. Vip-llava: Making large multimodal models understand arbitrary visual prompts. In *Proceedings of the IEEE/CVF Conference on Computer Vision and Pattern Recognition*, pages 12914–12923, 2024.
- [81] Jinze Bai, Shuai Bai, Shusheng Yang, Shijie Wang, Sinan Tan, Peng Wang, Junyang Lin, Chang Zhou, and Jingren Zhou. Qwen-vl: A frontier large vision-language model with versatile abilities. *arXiv preprint arXiv:2308.12966*, 2023.
- [82] Ke Li, Di Wang, Haojie Xu, Haodi Zhong, and Cong Wang. Language-guided progressive attention for visual grounding in remote sensing images. *IEEE Transactions on Geoscience and Remote Sensing*, 2024.
- [83] Tong Zhang, Yin Zhuang, He Chen, Guanqun Wang, Lihui Ge, Liang Chen, Hao Dong, and Lianlin Li. Posterior instance injection detector for arbitrary-oriented object detection from optical remote sensing imagery. *IEEE Transactions on Geoscience and Remote Sensing*, 2023.
- [84] Yin Zhuang, Yuqing Liu, Tong Zhang, Liang Chen, He Chen, and Lianlin Li. Heterogeneous prototype distillation with support-query correlative guidance for few-shot remote sensing scene classification. *IEEE Transactions on Geoscience and Remote Sensing*, 2024.
- [85] Minglang Qiao, Mai Xu, Lai Jiang, Peng Lei, Shijie Wen, Yunjin Chen, and Leonid Sigal. Hypersor: Context-aware graph hypernetwork for salient object ranking. *IEEE Transactions on Pattern Analysis and Machine Intelligence*, 46(9):5873–5889, 2024.